Psychophysical model of chromatic perceptual transparency based on subtractive color mixture

Franz Faul & Vebjørn Ekroll

Institut für Psychologie, Universität Kiel, Germany

Abstract

Variants of Metelli's episcotister model, which are based on additive color mixture, have been found to describe the luminance conditions for perceptual transparency very accurately. However, the findings in the chromatic domain are not that clear-cut, since there exist chromatic stimuli that conform to the additive model but do *not* appear transparent. We present evidence that such failures are of a systematic nature, and we propose an alternative psychophysical model based on subtractive color mixture. Results of a computer simulation revealed that this model approximately describes color changes that occur when a surface is covered by a filter. We present the results of two psychophysical experiments with chromatic stimuli, in which we directly compared the predictions of the additive model and the predictions of the new model. These results show that the color relations leading to the perception of a homogeneous transparent layer conform very closely to the predictions of the new model and deviate systematically from the predictions of the additive model.

1 Introduction

The phenomenon of perceptual transparency shows that the visual system is able to decompose the retinal image into a background and a transparent-layer component. Since local cone excitations provide no basis for such a decomposition, the visual system must, out of necessity, rely on relational information in the proximal stimulus. It has been found that the relation of four colors at X-junctions in the image is one important source of information that is used by the visual system to infer transparency and to determine the parameters of the transparent layer (Beck & Ivry, 1988; Beck, Prazdny, & Ivry, 1984; Da Pos, 1989; D'Zmura, Colantoni, Knoblauch, & Laget, 1997; Faul, 1996, 1997; Gerbino, Stultiens, Troost, & De Weert, 1990; Metelli, 1970, 1974).

Several models of perceptual transparency have been proposed that refer to this cue. Although these models differ in many respects, a broad distinction can be drawn between models of "additive" and of "subtractive" transparency. These two types of psychophysical models refer (heuristically) to different physical situations with grossly different image-generation processes. Nevertheless, it has been found that both situations may elicit perceptual transparency. Psychophysical models of additive transparency (Da Pos, 1989; D'Zmura et al., 1997; Gerbino et al., 1990; Metelli, 1974) refer to physical situations in which the colors in the region seen as transparent result from additive color mixture. A typical example of this case is a disk with an open sector (episcotister) rotating in front of a structured opaque background. Psychophysical models of subtractive transparency (Beck et al., 1984; Nakauchi, Silfsten, Parkinnen, & Usui, 1999; Westland & Ripamonti, 2000), on the other hand, refer to situations in which a structured opaque surface is seen through a light-transmitting object, for example a colored glass filter. In these cases subtractive color mixture is involved.

The fact that there exist two different types of psychophysical models for the same perceptual phenomenon naturally poses the question, which one gives a better description of perceptual transparency? The available empirical evidence provides no decisive answer to this question. This is due partly to the fact that until recently most studies on perceptual transparency considered only the achromatic case, in which the two types of model make almost identical predictions (Beck et al., 1984). Thus the support for the additive model found in studies on achromatic transparency (Gerbino et al., 1990; Kasrai & Kingdom, 2001) also supports subtractive models. Studies, in which psychophysical tests of the additive model in the chromatic domain were performed (Chen & D'Zmura, 1998; D'Zmura, Rinner, & Gegenfurtner, 2000; Faul, 1997; Hagedorn & D'Zmura, 2000) also, on the whole, supported this model. The fact that the additive model is commonly used in computer graphics to simulate color transparency (Foley, van Dam, Feiner, & Hughes, 1990) further supports the assumption that the predictions of this model can indeed not be too wrong.

One may thus be tempted to conclude that the empir-

ical evidence supports the additive model. It has been observed, however, that some stimuli that conform perfectly to the additive model are not perceived as transparent (Chen & D'Zmura, 1998; Da Pos, 1989). A possible interpretation of these deviations would be that the additive model describes only necessary but not sufficient conditions for perceptual transparency. On the basis of observations in their study, Chen and D'Zmura (Chen & D'Zmura, 1998) suggest, for example, that a further condition may be "that the color of the transparent overlay must share hue characteristics with both underlying surfaces". However, a different interpretation is also possible, namely, that the conditions of perceptual transparency are actually described by a subtractive model. From this perspective, the partial success of the additive model would be ascribed to a partial overlap of the predictions of both models (Beck et al., 1984).

In this paper we investigate the second interpretation. After presenting the additive model and a physically plausible filter model, we derive a simple approximation to the filter model, which depends solely on information directly available in the retinal image. This model will henceforth be referred to as the scaling model. In a computer simulation, we verified that the scaling model indeed closely approximates the filter model if restrictions of the natural environment are taken into account. The results of this simulation also revealed that the additive model and the scaling model make similar predictions in many cases. We present results of two psychophysical experiments with chromatic stimuli, in which we directly compared the predictions of the additive and the scaling model. These results show that the color relations that lead to the perception of a homogeneous transparent overlay deviate systematically from the predictions of the additive model and conform very closely to the predictions of the scaling model.

2 Models

The transparency models presented in this section refer to the four colors at an *X*-junction. Two adjacent colors with tristimulus vectors **A** and **B** correspond to the background surfaces in plain view, whereas the other two colors with tristimulus vectors **P** and **Q** correspond to the regions where **A** and **B**, respectively, are seen through a homogeneous transparent overlay.

2.1 Additive Model

There exist several almost identical variants of the additive model (Da Pos, 1989; D'Zmura et al., 1997; Faul, 1997). These models are straightforward extensions of the model of achromatic transparency that was originally proposed by Metelli (Metelli, 1970). Here, we refer to the convergence model of D'Zmura et al (D'Zmura et al., 1997). According to the convergence model, the four colors at an

X-junction should be optimal for an impression of transparency if the following relations hold:

$$\mathbf{P} = \alpha\mathbf{A} + (1-\alpha)\mathbf{F}, \tag{1}$$
$$\mathbf{Q} = \alpha\mathbf{B} + (1-\alpha)\mathbf{F} \tag{2}$$

with $0 < \alpha < 1$ and $F_i \geq 0$, $i = L, M, S$. It should be mentioned that the restriction on **F** is not part of the convergence model. We include it here, since empirical evidence suggests that stimuli that violate this condition are not perceived as transparent. Singh and Anderson (**?**) have recently shown this to be true in the achromatic case, and a reanalysis of Chen and D'Zmura's results (Chen & D'Zmura, 1998) of a test of the convergence model reveals that the subjects avoided settings that conformed to the convergence model but violated this additional constraint. Phenomenologically, the tristimulus vector **F** is putatively related to the perceived color of the transparent overlay and the scalar α is putatively related to the perceived "thickness" of the transparent layer.

The additive model is invertible, that is, if the four colors **A**, **B**, **P**, and **Q** are given, then the unknown parameters **F** and α can be calculated in the following way:

$$\alpha = (P_i - Q_i)/(A_i - B_i), \qquad i = L, M, S, \tag{3}$$
$$F_i = \frac{A_i Q_i - B_i P_i}{A_i - B_i - P_i + Q_i}. \tag{4}$$

2.2 Filter Model

The physical filter model (Allen, 1980; Nakauchi et al., 1999) that we will use as a starting point for the derivation of a psychophysical model (see section **2.2.3**) takes internal and external reflections into account. The three parameters of the filter are: (1) the absorption spectrum $m(\lambda)$ of the filter, (2) the filter thickness x, and (3) the refractive index $n(\lambda)$ of the filter material. For present purposes, the refractive index is assumed to be a constant function of wavelength, since it usually varies only slightly in the visible range of the spectrum. Typical filter materials such as glass and plastics have refractive indices in the range of 1.3 - 1.7.

If the absorption spectrum $m(\lambda)$ and the thickness x of the filter are given, then the inner transmittance $\theta(\lambda)$, i.e., the ratio of the amount of the light reaching the bottom of the filter to the amount entering at the top, can be calculated with Bouger's law: $\theta(\lambda) = \exp[-m(\lambda)x]$.

If the filter material has a refractive index that is different from that of air ($n_{air} \approx 1$), then each time the light crosses an air-filter boundary, a certain fraction k of the incident light does not pass the boundary but is reflected. The relative proportion k of direct reflection depends on the refractive indices of the two media, the angle of incidence, and the polarization of the light. It can be calculated from Fresnel's equations. If we assume unpolarized light and normal incidence, then these equations reduce to: $k = (n-1)^2/(n+1)^2$. For a typical glass filter with $n = 1.5$, we get, for example, $k = 0.04$.

Since direct reflection occurs at each air-filter interface, multiple inner reflections must be taken into account. Thus the total transmittance $t(\lambda)$, i.e., the relative amount of the incident light of wavelength λ that eventually leaves the bottom of the filter, is given by an infinite sum (see Fig. 1). The limiting value of this sum is:

$$t(\lambda) = \frac{(1-k)^2\theta(\lambda)}{1-k^2\theta^2(\lambda)}. \qquad (5)$$

Analogously, the total reflection $r(\lambda)$, i.e., the relative amount of the incident light of wavelength λ that is eventually reflected from the filter surface, is given by:

$$r(\lambda) = k + \frac{k(1-k)^2\theta^2(\lambda)}{1-k^2\theta^2(\lambda)}. \qquad (6)$$

Note that if $n = 1$ and therefore $k = 0$, then the total transmittance is identical to the inner transmittance $[t(\lambda) = \theta(\lambda)]$ and the total reflection $r(\lambda)$ vanishes.

The transmitted light $t(\lambda)$ then falls on the opaque background surface and is reflected back to the bottom of the filter surface, resulting in a new incident light at the bottom of the filter. The virtual reflectances $p(\lambda)$ and $q(\lambda)$ in the regions of the background covered by the filter can thus be determined by applying the above reasoning recursively (see Fig. 2). This results in (Beck et al., 1984; Brill, 1984)

$$p(\lambda) = \frac{t^2(\lambda)a(\lambda)}{1-r(\lambda)a(\lambda)} + r(\lambda) \qquad (7)$$

$$q(\lambda) = \frac{t^2(\lambda)b(\lambda)}{1-r(\lambda)b(\lambda)} + r(\lambda). \qquad (8)$$

Given an illumination spectrum $I(\lambda)$ and cone fundamentals $\phi_i(\lambda)$, $i = L, M, S$, we can calculate the four cone excitations **A**, **B**, **P** and **Q** from the (virtual) reflectance spectra $a(\lambda)$, $b(\lambda)$, $p(\lambda)$ and $q(\lambda)$ in the usual way: for instance, $A_i = \int a(\lambda)I(\lambda)\phi_i(\lambda)d\lambda$.
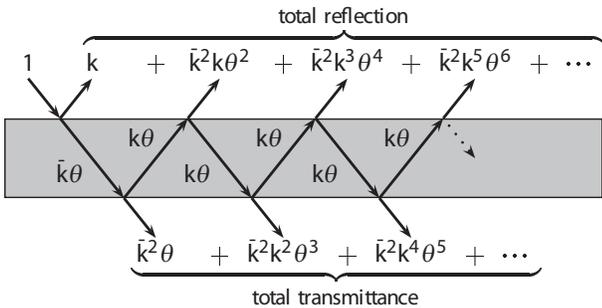

Figure 1: The pattern of internal reflections $[\bar{k} := (1-k)]$.

2.3 Scaling Model

In this subsection we propose a novel psychophysical model of color transparency, which we refer to as the scaling model. It states that the four cone excitations **A**, **B**, **P**
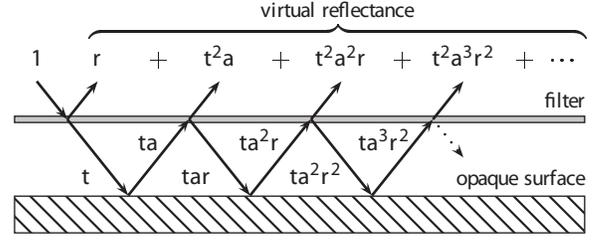

Figure 2: The pattern of external reflections. An opaque surface with reflectance $a(\lambda)$ is assumed.

and **Q** at an *X*-junction should be optimal for an impression of transparency if the following relations hold:

$$P_i = \beta_i(A_i + \kappa I_i), \qquad (9)$$
$$Q_i = \beta_i(B_i + \kappa I_i), \qquad (10)$$

with $I_i = (A_i + B_i)/2$, $0 < \beta_i < 1$, and $\kappa \geq 0$.

The scaling model has the same number of unknown parameters as the additive model and is likewise invertible. If the cone excitations **A**, **B**, **P** and **Q** are given, then the unknown parameters β_i, $i = L, M, S$, and κ can be calculated in the following way[1]:

$$\beta_i = (P_i - Q_i)/(A_i - B_i), \qquad (11)$$

$$\kappa = \frac{2(Q_iA_i - P_iB_i)}{(P_i - Q_i)(A_i + B_i)}. \qquad (12)$$

The scaling model may be understood as a rough approximation to the filter model presented above; in the sense that the scaling model approximately describes the changes in color codes that occur when a bipartite background is covered by a physical filter that conforms to the filter model. To show this, we first approximate the filter equations following the approach of Nakauchi et al (Nakauchi et al., 1999): We neglect the denominators in Eqs. (5) and (6), which are normally close to 1. Thus $t(\lambda) = (1-k)^2\theta(\lambda)$ and $r(\lambda) = k + k(1-k)^2\theta^2(\lambda)$. If we solve the approximation of $t(\lambda)$ for $\theta(\lambda)$ and substitute the result into the approximation of $r(\lambda)$, we get $r(\lambda) = k + kt^2(\lambda)/(1-k)^2$. Since $(1-k)^2$ is close to 1 for typical refractive indices, it may also be neglected, and thus we obtain $r(\lambda) = k[1 + t^2(\lambda)]$. We also neglect the third order terms in Eqs. (7) and (8), thus

$$p(\lambda) = t^2(\lambda)a(\lambda) + r(\lambda), \qquad (13)$$
$$q(\lambda) = t^2(\lambda)b(\lambda) + r(\lambda). \qquad (14)$$

Substituting the approximation of $r(\lambda)$ leads to

$$p(\lambda) = t^2(\lambda)[a(\lambda) + k] + k, \qquad (15)$$
$$q(\lambda) = t^2(\lambda)[b(\lambda) + k] + k. \qquad (16)$$

---

[1]A minor drawback of this formulation is that Eq. (11) may be undefined for some i. This problem is easily solved: Choose i such that $A_i - B_i > 0$ (this is always possible, since at an *X*-junction we have **A** $\neq$ **B**) and calculate κ for this coordinate using Eq. (12). Then $\beta_i = P_i/(A_i + W_i)$, with $W_i = \kappa(A_i + B_i)/2$.

In order to relate the reflectances $a(\lambda)$, $b(\lambda)$, $p(\lambda)$ and $q(\lambda)$ to the corresponding cone excitations $\mathbf{A}$, $\mathbf{B}$, $\mathbf{P}$, and $\mathbf{Q}$ that result under a certain illumination $I(\lambda)$, we consider the special case $k = 0$. For this case, the results of a computer simulation performed by Westland and RipamontiWestland and Ripamonti (2000) indicate that $P_i/Q_i = A_i/B_i$ holds to a reasonable approximation if smooth spectra are used. Such spectra are typically found in natural environments. This means that the effect of the spectral multiplication of $a(\lambda)$ and $b(\lambda)$ with $t^2(\lambda)$ on the cone excitations can be approximated by a scalar multiplication of the cone excitations A_i and B_i with appropriate factors β_i, $i = L, M, S$. Since $t^2(\lambda) \leq 1$, it can further be concluded that $0 \leq \beta_i \leq 1$. A similar result has been reported for illuminations (Nascimento & Foster, 1997), i.e., the effect of multiplying reflectance spectra $x(\lambda)$, $y(\lambda)$ by an illumination spectrum $I(\lambda)$ on the cone excitations can be approximated by a multiplication of the corresponding cone excitations X_i, Y_i by appropriate scalar factors $I_i > 0$.

Using these results and assuming an illumination $I(\lambda)$, we can formulate psychophysical counterparts for Eqs. (15) and (16) in terms of the cone excitations $\mathbf{A}$ and $\mathbf{B}$, "illumination factors" I_i, and "transmittance factors" β_i:

$$P_i = \beta_i(A_i + kI_i) + kI_i, \qquad (17)$$
$$Q_i = \beta_i(B_i + kI_i) + kI_i, \qquad (18)$$

with $k \geq 0$, $0 \leq \beta_i \leq 1$, and $I_i > 0$, $i = L, M, S$.

The illumination factors in Eqs. (17) and (18) are unknown and must be estimated from the visual array. In principle, there are many ways to do this, and each different alternative would lead to a slightly different psychophysical model. In the scaling model, we assume that the arithmetic mean of the background colors is used to estimate $\mathbf{I}$ up to a scalar intensity factor $s > 0$, i.e., for the case with two background colors $\mathbf{A}$ and $\mathbf{B}$, we get $\mathbf{I} = s(\mathbf{A} + \mathbf{B})/2$. Formally, this is a kind of "gray world assumption" (D'Zmura, Iverson, & Singer, 1995). If we further neglect the last term kI_i in Eqs. (17) and (18), we finally get Eqs. (9) and (10) of the scaling model. A comparison of Eqs. (17) and (18) with Eqs. (9) and (10) of the scaling model reveals that the parameter κ of the scaling model stands for $k \cdot s$, where s is the unknown intensity scaling factor for the illumination $\mathbf{I}$. It should be noted that the parameter restrictions for β_i and κ given above are derived from the interpretation of the model as an approximation of the filter model. These restrictions are probably too lenient and need further refinement.

Casual observations indicate that the parameters of the model relate to the perceived quality of the filter in roughly the following way: The ratios of the scaling parameters β_i are correlated with the perceived color of the filter. The vector $\boldsymbol{\beta} = (0.5, 0.7, 0.5)$ would, for example, correspond to a greenish filter, whereas a filter defined by $\boldsymbol{\beta} = (0.7, 0.5, 0.5)$ would appear reddish. The absolute size of the vector $\boldsymbol{\beta}$ correlates inversely with the perceived thickness of the filter. A filter given by the vector $\boldsymbol{\beta} = (0.25, 0.35, 0.25)$, for example, appears thicker than

the filter defined by $\boldsymbol{\beta} = (0.5, 0.7, 0.5)$. The remaining parameter κ is related to the "perceived haziness" of the filter. For $\kappa = 0$, the filter looks like clear colored glass. With increasing κ, the filter looks more whitish, like a milky colored glass.

3   Numerical Experiment

Since there are quite a number of approximations in the derivation of the scaling model, we investigated, in a computer simulation, how good the approximation to the filter model really is if we take regularities of natural reflectance spectra into account.

3.1   Methods

The filter model described above was used to simulate the four cone excitations at an X-junction. We used frequency-limited spectraStiles, Wyszecki, and Ohta (1977); Wyszecki and Stiles (1982) to simulate reflectance and absorption spectra. Frequency-limited spectra are smoothly varying functions of wavelength that are quite representative of natural reflectance spectra. They are defined by $\rho(\lambda) = [1 + \vartheta(\lambda)]/2$ with

$$\vartheta(\lambda) = \sum_{i=-l}^{l} \tau_i \operatorname{sinc}^2[\pi\omega(\lambda - \lambda_0) - i\pi/2] \qquad (19)$$

and $-0.5 \leq \tau_i \leq 0.5$. In the simulation, we set the (uncritical) "zero adjustment" parameter λ_0 to 350nm. The definition requires $l = \infty$ to suppress all frequency components above the limiting frequency, but for practical purposes a value of $l = 50$ leads to a good approximation. If all other parameters are fixed, then each member of this set of frequency-limited spectra is defined by a specific choice for τ_i, $i = \pm 1, \dots, \pm 50$. To draw random samples, we set these weights to random values. The most interesting parameter is ω, since it represents the limiting frequency and thus controls the smoothness of the spectrum. It has been found that the limiting frequency of natural spectra typically lies inside the range of $1/100$–$1/50$ cycles/nm (Maloney, 1986). In line with these findings, we set $\omega = 1/75$ cycles/nm for reflectances $a(\lambda)$, $b(\lambda)$. To simulate absorption spectra $m(\lambda)$, we used $\omega = 1/150$ cycles/nm. In addition, each simulated reflectance spectrum was multiplied by a random number from the interval $[0, 1]$ to increase the range of background luminances in our sample, and each absorption spectrum was rescaled to the min/max-range $[0.1, 0.9]$ to obtain relatively saturated filter colors. The thickness of the filter was set to $x = 0.7$, and the refractive index n was varied in four steps: $n \in \{1, 1.2, 1.4, 1.6\}$. We chose the CIE daylight illuminant D_{65} as illumination (Wyszecki & Stiles, 1982). The cone fundamentals given by Stockman and SharpeStockman and Sharpe (2000) were used to calculate cone excitations $\mathbf{A}$, $\mathbf{B}$, $\mathbf{P}$ and $\mathbf{Q}$. All spectra were defined from 400 to 700 nm in 5 nm steps.

For each of the four refractive indices, 500 stimuli were calculated. Then both the additive and the scaling model were fitted to each stimulus according to a least-square criterion. In the case of the additive model, we searched for parameters $0 \leq \alpha \leq 1$ and $F_i \geq 0$, $i = L, M, S$, such that $E_a = ||\mathbf{P}_a - \mathbf{P}||^2 + ||\mathbf{Q}_a - \mathbf{Q}||^2$ was minimal, with $\mathbf{P}_a$ and $\mathbf{Q}_a$ calculated according to Eqs. (1) and (2). For the scaling model, we searched for model parameters $0 \leq \beta_i \leq 1$, $i = L, M, S$, and $\kappa \geq 0$, such that $E_s = ||\mathbf{P}_s - \mathbf{P}||^2 + ||\mathbf{Q}_s - \mathbf{Q}||^2$ was minimal, with $\mathbf{P}_s$ and $\mathbf{Q}_s$ calculated according to Eqs. (9) and (10).

3.2 Simulation Results

To evaluate the goodness of the fits for both models, we calculated for each coordinate i, $i = L, M, S$, the relative deviation

$$E_i^r := |\hat{X}_i - X_i| / X_i \qquad (20)$$

of the estimated cone excitations from those that resulted from the filter simulation. In Eq. (20), $\mathbf{X}$ stands for an element of $\{\mathbf{P}, \mathbf{Q}\}$ and $\hat{X}$ for an element of $\{\mathbf{P}_s, \mathbf{Q}_s\}$ or $\{\mathbf{P}_a, \mathbf{Q}_a\}$, respectively. All E_i^r for a certain n were pooled over all coordinates of $\mathbf{P}$ and $\mathbf{Q}$ for each model. Figure 3 shows the cumulative relative frequency of E^r for different refractive indices n. It can be seen that the scaling model approximates the filter model very closely. For all refractive indices n, more than 96% of all 3000 cone excitations deviate less than 10% from those predicted by the filter model. The approximation of the scaling model is always clearly better than that of the additive model, but the difference between the two models decreases with increasing n. The latter result can be explained by reference to Eqs. (7) and (8) of the filter model, which show that $p(\lambda)$ and $q(\lambda)$ share a common additive component $r(\lambda)$. The size of this component is 0 for $k = 0$, i.e., $n = 1$, and increases monotonically with k and therefore also with n (see Eq. (6)). Since this additive component can be perfectly fitted by the additive model, it is to be expected that it performs better in cases with large n, where the common additive component $r(\lambda)$ is substantial. The difference between the two models would have been even smaller, if we had used less-saturated filter colors in the simulation. Obviously, there is a large overlap in the predictions of the scaling model and those of the additive model. Thus a partial success of the additive model in predicting perceptual transparency is to be expected even if the conditions of perceptual transparency are actually described by a subtractive model.

Now we will briefly discuss the relationship of these findings to the results of Westland and Ripamonti (2000). In their study they used a simplified physical model of transparency to simulate cone excitations $\mathbf{A}$, $\mathbf{B}$, $\mathbf{P}$, and $\mathbf{Q}$ at X-junctions and found approximately $P_i / Q_i = A_i / B_i$, $i = L, M, S$. On the basis of this result, they hypothesized that constant cone-excitation ratios may be used by the visual system as a cue to detect transparency (ratio model).
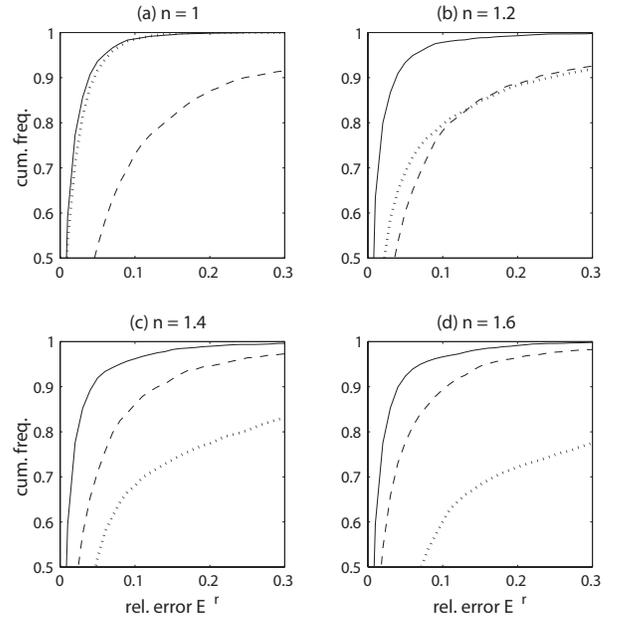

Figure 3: The cumulative relative frequency of relative deviations E^r of the predictions of different psychophysical models from the predictions of the physical filter model for different refractive indices n. The solid, dashed, and dotted curves show the deviations of the scaling model, the additive model, and the ratio model, respectively.

The physical model they used is essentially identical to the special case $n = 1$ (or, equivalently, $k = 0$) of the more general filter model presented above. In terms of the scaling model this means that $\kappa = 0$. The scaling model then reduces to $P_i = \beta_i A_i$, $Q_i = \beta_i B_i$, i.e., it predicts constant cone-excitation ratios. In the simulation, we found for $n = 1$ a mean κ of 0.033, which is indeed close to zero. This implies that the constant-cone-excitation-ratio criterion is approximately fulfilled in this case. However, for $n = 1.2, 1.4, 1.6$, where the scaling model approximates the filter model just as well as for $n = 1$, we found mean κ's of 0.179, 0.468, 0.920 respectively, which means that in these cases the constant-cone-excitation-ratio criterion is violated. Only in the special case $n = 1$ is the transparency criterion proposed by Westland and Ripamonti consistent with the scaling model. In order to allow a direct comparison of the approximation of the ratio model with the approximations of the additive and scaling models, we also fitted the ratio model to the simulated data. That is, we searched for parameters $\gamma_i > 0$, $i = L, M, S$, such that $E_r = ||\mathbf{P}_r - \mathbf{P}||^2 + ||\mathbf{Q}_r - \mathbf{Q}||^2$ was minimal, where $\mathbf{P}$ and $\mathbf{Q}$ are the cone-excitations from the simulation and $P_{ri} = \gamma_i A_i$, $Q_{ri} = \gamma_i B_i$ are the predictions of the ratio model. The results are shown in Fig. 3. It can be seen that the scaling model approximates the data just as well as the scaling model for $n = 1$, as expected, but that the deviations increase rapidly with increasing n. For larger n, the ratio model is also outperformed by the additive model.

4 Psychophysical Experiments

We designed two psychophysical experiments to investigate whether the additive model or the scaling model predicts perceptual transparency more successfully. Such tests are complicated by a fact clearly demonstrated by the results of the simulation study, namely that the predictions of the two models are very similar in many cases. It is therefore necessary to select stimuli for which the two models make distinctly different predictions.

We identified tristimulus vectors $\mathbf{A}$, $\mathbf{B}$ and $\mathbf{P}$, such that the additive and the subtractive model predict unique and distinctly different settings $\mathbf{Q}_a$ and $\mathbf{Q}_s$, respectively, for the remaining tristimulus vector $\mathbf{Q}$. The task of the subjects was to find the position on the line through $\mathbf{Q}_a$ and $\mathbf{Q}_s$ that optimizes the impression of transparency. Thus the two models could be compared according to a clear criterion: If the conditions for optimal perceptual transparency are described by the additive model, then it is to be expected that the subjects will choose the point $\mathbf{Q}_a$. If they are instead described by the scaling model, then the subjects should choose $\mathbf{Q}_s$.

5 Experiment 1

In experiment 1, we investigated the case of a chromatic transparent overlay in front of an achromatic background. The fixed colors $\mathbf{A}$, $\mathbf{B}$, and $\mathbf{P}$ were determined in the following way: We chose two different achromatic colors $\mathbf{A}$ and $\mathbf{B}$, i.e. $\mathbf{B} = s\mathbf{A}$, $s \neq 1$, a chromatic "filter color" $\mathbf{F}$, and a certain α between 0 and 1. The fixed color $\mathbf{P}$ was then calculated according to the additive model: $\mathbf{P} = \alpha\mathbf{A} + (1-\alpha)\mathbf{F}$. The path in color space on which the subjects could search for the remaining color $\mathbf{Q}$ that optimizes their impression of transparency was restricted to the line segment $\overline{\mathbf{BF}}$. The search was done by adjusting a parameter γ between 0 and 1 that was then used to calculate $\mathbf{Q} = \gamma\mathbf{B} + (1-\gamma)\mathbf{F}$. Under these conditions, the additive model predicts that the subjects will choose $\gamma = \alpha$. The scaling model, on the other hand, predicts (cf. Appendix A.1) that they will choose

$$\gamma = \frac{\alpha}{\alpha + s - \alpha s}. \tag{21}$$

5.1 Methods

We used six colors $\mathbf{F}$ that can be roughly described as red, green, blue, yellow, magenta, and cyan. Each of them was combined with an achromatic ($x = 0.29$, $y = 0.31$) color $\mathbf{A}$, which was either incremental or decremental to $\mathbf{F}$ in luminance. The CIE 1931 $2°$ xyL-coordinates of $\mathbf{F}$ and the luminances of $\mathbf{A}$ are listed in Table 1. Each of the 12 resulting pairs $(\mathbf{A}, \mathbf{F})$ was then combined with one of five achromatic colors $\mathbf{B}$ with luminances 5.0, 14.9, 24.8, 34.6, and 44.5 cd/m^2. For each of the 60 $\mathbf{A}$, $\mathbf{B}$, $\mathbf{F}$ triples, one of the three values 0.3, 0.5, 0.7 for α was used to calculate $\mathbf{P}$. In this way, we got 180 stimuli with fixed colors $\mathbf{A}$, $\mathbf{B}$, $\mathbf{P}$.

Table 1: CIE 1931 $2°$ xyL-values for layer color $\mathbf{F}$ and luminances of the background color $\mathbf{A}$. Luminances are given in cd/m^2.

Color	red	green	blue	yellow	magenta	cyan
F						
x	0.43	0.29	0.20	0.35	0.29	0.24
y	0.32	0.48	0.16	0.42	0.22	0.31
L	13.20	27.00	10.00	20.00	11.60	18.50
A						
inc	9.20	18.80	7.10	14.00	8.10	12.80
dec	17.20	35.00	13.00	26.00	15.10	24.10

Figure 4: The stimulus configuration used in Exp. 1. In the experiment, the stimuli were chromatic.

Figure 4 depicts the stimulus configuration used in experiment 1. Each of the 16 squares in this stimulus had an edge length of 5 cm ($2.29°$ visual angle). The stimuli were presented in the center of a 20-in CRT monitor (Sony GDM-20SE2T5) on a black background. The monitor was located at one end of a box, which was painted matte black inside. The subjects viewed the screen through a hole on the other side of this box. A black silicon cuff similar to that of a diving mask ensured that no residual light from outside the box could enter the subject's eyes. The viewing distance was 125 cm. The monitor was controlled by a graphics card (ELSA Gloria) with a color depth of 8 bits per RGB-channel. This setup was colorimetrically calibrated by means of a colorimeter (LMT C1210) following a standard procedure described by Brainard (1989)

For each stimulus the subjects had to perform a two-step procedure. In step 1, they used two keys on a keyboard to adjust the parameter γ that determined the color $\mathbf{Q}$ as described above. They were instructed to choose $\mathbf{Q}$ such that their impression of transparency was optimal, in the sense that the transparent layer appeared to be maximally homogeneous and that the colors seen behind the layer were maximally similar to the background colors $\mathbf{A}$ and $\mathbf{B}$. In step 2, they rated the goodness of the transparency impression for the stimulus generated in this way, using a scale from 0 to 5, where 0 denotes "no transparency" and 5 "optimal transparency".

Three subjects participated in the experiment, one of them being the second author (VE). All had normal color vision and normal visual acuity, and were experienced psychophysical observers. Subject VE performed the ex-

periment once; the other two subjects performed it twice. Thus five settings were collected per data point.
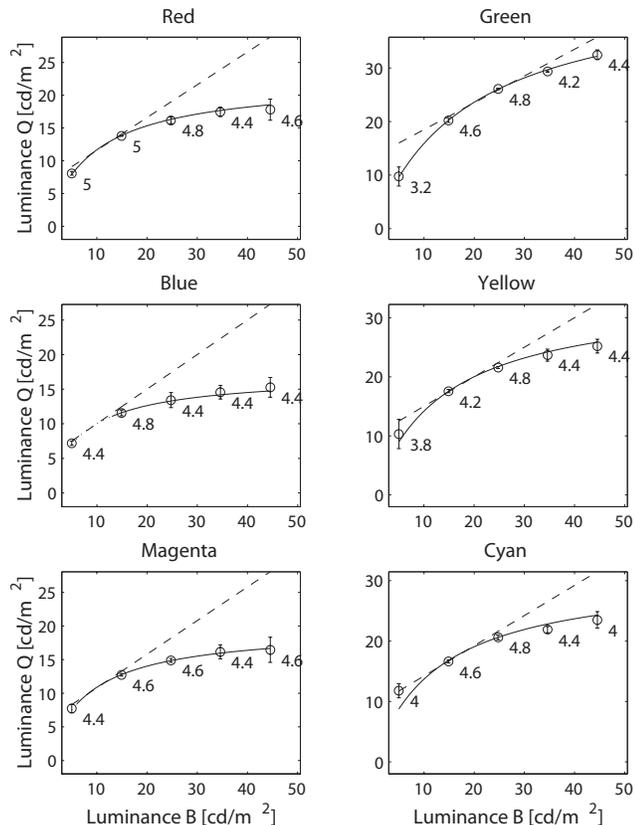
5.2 Results

Figure 5: Results for the condition $\alpha = 0.5$ and **F** incremental in luminance relative to **A**. The mean settings are shown by open dots. The error bars enclose the 95% confidence interval of the mean. The dashed lines show the prediction of the additive, the solid lines that of the scaling model. The dotted parts of the prediction curve of the scaling model (blue condition) denote (slight) violations of the condition $\beta_i < 1$. The numbers at each data point are mean transparency ratings for the corresponding stimulus.
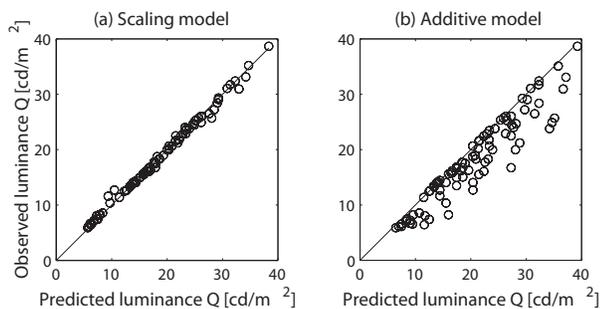

Figure 6: Predicted vs. observed luminance of **Q** for both models.

Since **Q** by definition is a convex mixture of the colors **B** and **F**, we can refer to the luminance values to evaluate how well the subjects settings comply with the predictions of each model. Figure 5 shows in detail the results for the condition "$\alpha = 0.5$" and "**F** incremental in luminance relative to **A**". It can be seen that the subjects made highly reliable settings. The mean settings of the subjects closely match the predictions of the scaling model and deviate systematically from those of the additive model. The mean transparency ratings that are close to the maximal value 5 demonstrate that the subjects had indeed a near-optimal impression of transparency. There seems to be a small trend in the ratings for the "goodness of transparency". A simple explanation for this trend may be that the subjects, although instructed otherwise, were not always able to completely ignore the perceived quality of the filter. The scaling model predicts that both the perceived thickness and the perceived haziness of the filter should increase with increasing luminance of **B**. The trend in the ratings of the subjects may thus indicate a slight preference for stimuli with medium values for perceived thickness and perceived haziness.

The results for the other conditions are very similar to the subset shown in Fig. 5. We present these results only in a more condensed form to save space. In Fig. 6 the luminance of **Q** predicted by the models is plotted against the mean observed luminance for all stimuli. Obviously, the observed **Q**'s comply much better with the predictions of the scaling model ($R^2 = 0.994$) than with those of the additive model ($R^2 = 0.889$). The special form of the deviations can easily be understood by referring to Fig 5. We should add that the ratio model, which is not shown graphically, performed even worse ($R^2 = 0.646$). The transparency rating was high for all stimuli ($m = 4.25, sd = 0.64$). This indicates that the impressions of transparency were compelling throughout.

6 Experiment 2

The second experiment was similar to the first, except that we investigated the more general case in which the background colors **A** and **B** are not required to be isochromatic. In this case, the colors **A**, **B**, and **P** and one of the coordinates of the color **Q** were fixed. Under these conditions, both models uniquely predict how the two remaining coordinates of **Q** have to be chosen to fulfill the model equations. The general approach was to generate a random set of fixed colors for which the prediction of the additive model ($\mathbf{Q}_a$) and the prediction of the scaling model ($\mathbf{Q}_s$) were distinctly different. The path on which the subjects had to search for a **Q** that optimizes their impression of transparency was then restricted to the line in color space through $\mathbf{Q}_a$ and $\mathbf{Q}_s$.
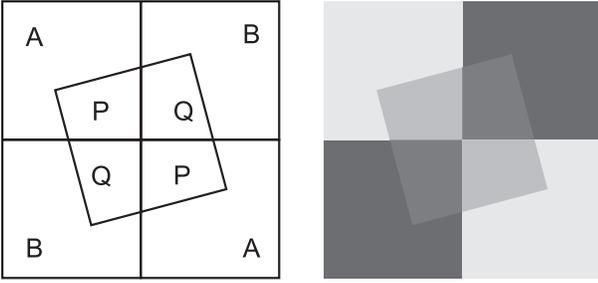
Figure 7: The stimulus configuration used in Exp. 2 with an achromatic example. In the experiment, the stimuli were chromatic.

6.1 Methods

To determine the fixed colors **A**, **B**, and **P**, we first chose random samples for **A** and **B**, and one of six layer colors **F**, $\alpha = 0.4$, and then calculated **P** according to Eq. (1) of the additive model. The background colors **A** and **B** were calculated from random samples from the set of frequency-limited spectra (see Subsection **3.3.1**) with $\omega = 1/50$ cycles/nm, which were afterward multiplied by a random number between 0 and 1 to get a wider range of background luminances. The layer colors **F** were calculated from Munsell chip spectraParkkinen, Hallikainen, and Jaaskelainen (1989) (see Table 2) that appear approximately red, green, blue, yellow, magenta, and cyan under daylight illumination. As illumination, we used the CIE daylight spectrum D_{65} (Wyszecki & Stiles, 1982) that was scaled appropriately with a scalar factor to get luminances inside the monitor gamut. In order to calculate the cone excitations **A**, **B**, and **F**, we used the $2°$ cone fundamentals given by Stockman and SharpeStockman and Sharpe (2000) that were appropriately scaled following an approach of Golz and MacLeodGolz and MacLeod (submitted) (see Appendix A.3). We then chose that coordinate i of **Q** to be fixed that is presumed to be the least important to code the layer color (see Table 2). This coordinate Q_i was then set to a value that ensured $\kappa = 0.5$ for the scaling model:

$$Q_i = \frac{A_i\kappa + B_i(2+\kappa)}{B_i\kappa + A_i(2+\kappa)}P_i. \qquad (22)$$

Given these fixed values ($\mathbf{A}$, $\mathbf{B}$, $\mathbf{P}$, Q_i), the uniquely determined predictions $\mathbf{Q}_a$, $\mathbf{Q}_s$, with $Q_{ai} = Q_{si}$, were calculated (see Appendix A.2).

In this way, a large number of colors **A**, **B**, **P**, $\mathbf{Q}_a$, and $\mathbf{Q}_s$ were generated for each layer color. From each of these sets, we drew a random sample of 15 stimuli that fulfilled the following criteria: (a) luminances of **A** and **B** ≥ 5 cd/m^2, (b) $P_i/A_i \leq 1$, (c) $||\mathbf{Q}_a - \mathbf{Q}_s|| > c$, with c as given in Table 2, (d) euclidean distances between $\mathbf{Q}_a$ and $\mathbf{Q}_s$ in the CIE UCS 1976 uv-chromaticity spaceWyszecki and Stiles (1982) ≥ 0.02, (e) all parameters of both models lie in the admissible range, (f) all colors are inside the monitor gamut. This results in 90 different stimuli. All

Table 2: Munsell chips for layer color **F**, fixed channel in **Q** and minimal LMS-distance between $\mathbf{Q}_a$ and $\mathbf{Q}_s$ (see text).

Layer **F**	Munsell	fixed	$c = \min\lVert\mathbf{Q}_a - \mathbf{Q}_s\rVert$
red	5R 6/10	S	1
green	10GY 6/10	S	1
blue	5PB 6/10	L	5
yellow	5Y 8/8	S	1.5
magenta	10P 6/10	M	1
cyan	10BG 6/8	L	1

colors of the stimuli were then transformed to XYZ coordinates by using the transformation matrix described by Golz and MacLeodGolz and MacLeod (submitted) (see Appendix A.3). The search path for **Q** was the line in color space that connects $\mathbf{Q}_a$ and $\mathbf{Q}_s$. This line was clipped at the boundaries of the monitor gamut.

The procedure we used to generate the stimuli was motivated by several considerations: First, we tried to ensure that $\mathbf{Q}_a$ and $\mathbf{Q}_s$ were perceptually sufficiently different from each other to allow a clear decision between the two models [criteria (c) and (d)]. A second consideration was to choose parameter values for both models that were not too close to the boundary values [$\alpha = 0.4$ to calculate **P** and $\kappa = 0.5$]. A third goal was to ensure that the colors in the stimulus would be physically plausible [calculation of **A**, **B**, and **F** from spectra and criteria (a) and (b)]. A further goal was to generate a wide range of colors [use of six clearly different saturated colors for **F** and random samples for **A** and **B**].

Figure 7 depicts the stimulus configuration used in experiment 2. The edge length of the outer square was 17 cm, that of the inner square 8.5 cm ($7.78°$, $3.89°$ visual angle). Apparatus and calibration procedure were the same as in experiment 1. The task of the subjects was also essentially the same, except that the parameter γ, which they adjusted in step 1 of the procedure, determined the position between the two end points of the adjustment line through $\mathbf{Q}_a$ and $\mathbf{Q}_s$.

Four subjects participated in the experiment. Three of them had already participated in experiment 1, including one of the authors (VE). All had normal color vision and normal visual acuity, and were experienced psychophysical observers. Each subject performed the experiment five times. This results in 20 settings for each of the 90 data points.

6.2 Results

Figure 8 shows the relative position of the mean settings on the adjustment line for different layer colors. It can be seen that the mean settings comply rather closely with the predictions of the scaling model and deviate systematically from the predictions of the additive model. Figure 9 gives a different representation of the data that facilitates the estimation of the absolute size of the deviations.
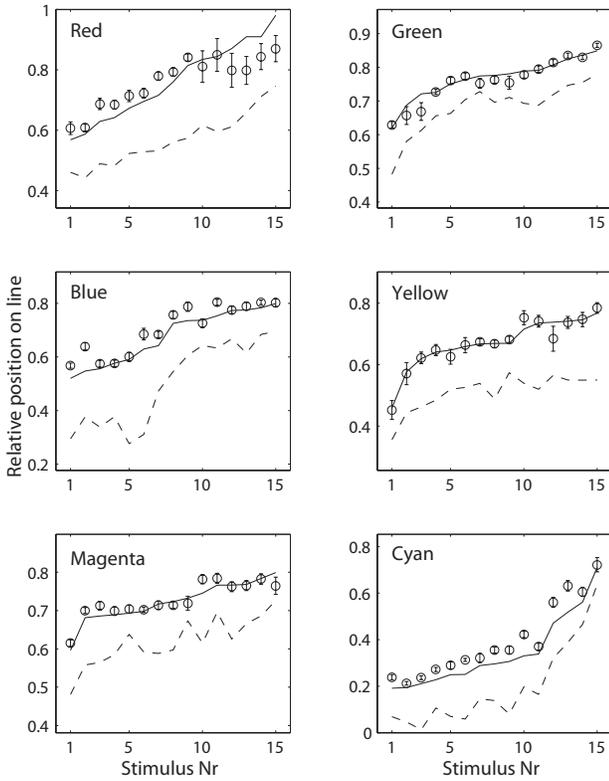
Figure 8: Mean adjustments for **Q**. Relative positions γ along the adjustment line are shown. The solid line connects the predictions of the scaling model, the dashed line the predictions of the additive model. The error bars enclose the 95% confidence interval of the mean. (Stimuli are sorted for increasing rel. position of Q_s.)

Figure 9: Deviations from the predictions of both models. The plots in the upper row show the deviations of the mean settings from the predictions in the CIE 1976 UCS *uv*-color space. The plots in the lower row show the deviations of the mean luminances from the predicted luminances.

It shows that the difference between predicted and mean observed CIE 1976 UCS *uv* coordinates is always less than 0.02 for the scaling model and approximately three times greater for the additive model. The mean luminance settings also comply much better with the predictions of the scaling model ($R^2 = 0.994$) than with those of the additive model ($R^2 = 0.834$). In Fig. 10 the means of the observed cone excitations are plotted against the predicted cone excitations for both models. We found $R_L^2 = 0.993$, $R_M^2 = 0.994$, $R_S^2 = 0.968$ for the scaling model, and $R_L^2 = 0.824$, $R_M^2 = 0.856$, $R_S^2 = 0.663$ for the additive model. This analysis reveals that the greatest deviation from the predictions of the scaling model are found in the *S* channel. The transparency ratings of the subjects were high throughout ($m = 4.1, sd = 0.495$). In summary, the data of experiment 2 are in line with the findings of experiment 1. In both cases, the scaling model predicts the color relations for optimal perceptual transparency better than the additive model.

Although the data of experiment 2 clearly favor the scaling model, there seem to be some small systematic errors. However, this does not necessarily speak against the validity of the scaling model, since there are several poten-
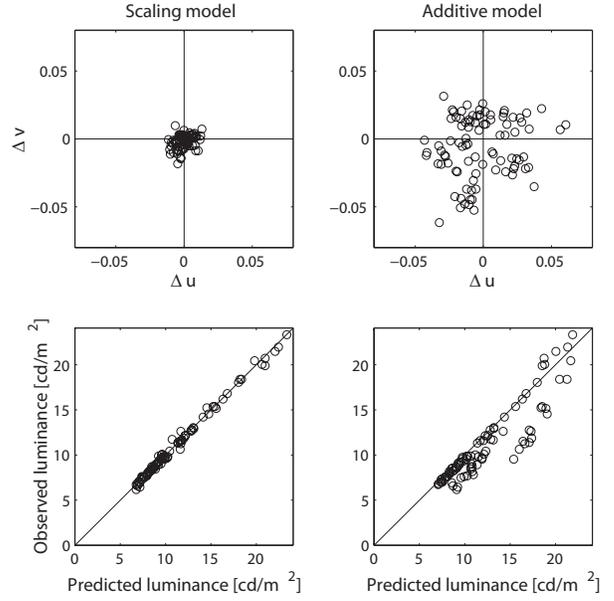
tial sources of systematic error that may explain these deviations. First, a systematic error may result from imprecisions of the monitor calibration. It is well known that CRT monitors show systematic intensity dropoffs at the edges of the screen (we calibrated only in the center of the screen). Further, imprecisions in the cone fundamentals may have negatively influenced the precision of the predictions, since the calculation of the predictions of the scaling model relies critically on this data. In addition, individual differences in cone sensitivities and transparency criteria may in part be responsible for systematic deviations from the predictions of the scaling model. The mean settings of the subjects did indeed deviate among one other almost as much as did the grand mean from the predictions of the scaling model.

7   Summary and Discussion

The work presented in this paper started from the observation that the additive model of perceptual transparency predicts perceived transparency in cases where it is not perceived. We explored the hypotheses that these are systematic failures of the model and that the conditions for perceptual transparency are better described by a subtractive model. The preference for additive models in previous psychophysical investigations may in part be due to their simplicity. Indeed, it is hardly conceivable that transparency mechanisms of the visual system are based on a physically realistic model of filter transparency. However, we have provided evidence that basic properties of sub-
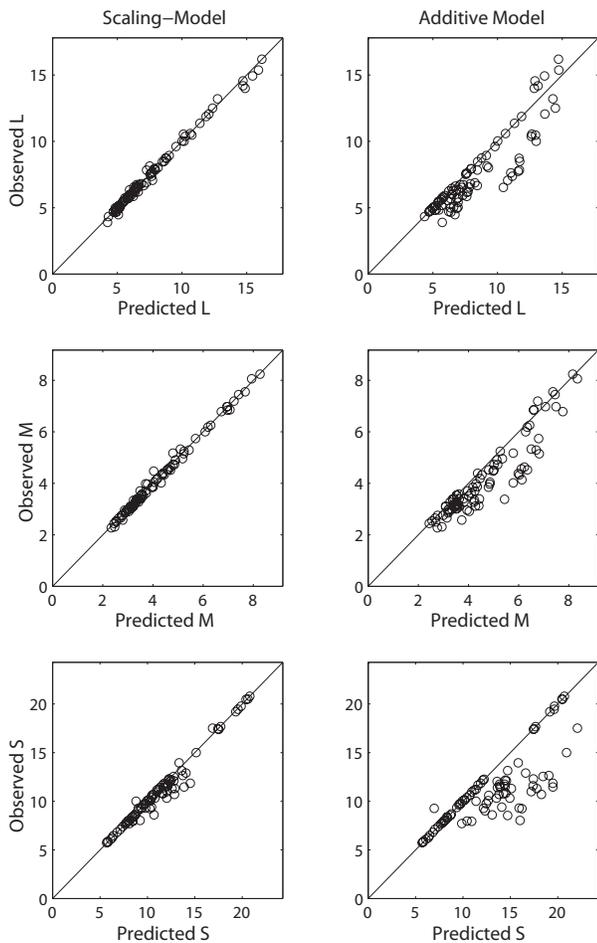
Figure 10: Predicted vs. observed cone excitations for both models. Note that some of the points represent experimentally fixed coordinates and are therefore, by necessity, perfectly predicted by both models.

tractive mixtures can be described with a relatively simple model (scaling model), if we take regularities in the natural environment into account. We have further shown that there is a considerable overlap of the predictions of subtractive and additive models. If we assume that the true conditions for perceptual transparency are described by a subtractive model, then this finding could explain why the additive model proved to be a useful heuristic to predict transparency for practical purposes, e.g. computer graphics applications.

Comparison of the Scaling Model with Extant Models

The results of the two psychophysical experiments that were conducted to directly compare the predictions of the additive and the scaling model clearly support the latter model. In both experiments, the settings of the subjects closely followed the predictions of the scaling model and deviated systematically from those of the additive

model. The high transparency ratings of the subjects confirm that the stimuli predicted by the scaling model are in fact perceived as transparent. This suggests that the failures of the additive model are indeed of a systematic nature and cannot be amended by assuming additional constraints, as, for example, the one suggested by Chen and D'ZmuraChen and D'Zmura (1998) "that the color of the transparent overlay must share hue characteristics with both underlying surfaces".

It is natural to ask whether the scaling model avoids predicting transparency in those cases in which Chen and D'ZmuraChen and D'Zmura (1998) found violations of the convergence model. To investigate this, we reanalyzed their data. This analysis revealed that there are apparently two qualitatively different types of violations. The first type concerns stimuli in which some of the coordinates of the convergence point **F** are negative. As mentioned in subsection **2.2.1**, the condition $F_i \geq 0$, $i = L, M, S$, is not part of the convergence model, and stimuli with $F_i < 0$ are therefore valid with respect to that model. However, it has recently been shown that this restriction on **F** is a necessary condition for perceptual transparency in the achromatic case (**?**). The finding of Chen and D'Zmura that their subjects avoided such stimuli indicates that it is also a necessary condition in the chromatic case. Since stimuli that violate the condition $F_i \geq 0$, $i = L, M, S$, of the additive model in almost all cases also violate the condition $\kappa \geq 0$ of the scaling model, we conclude that the scaling model avoids wrong predictions of that kind. However, some of the violations reported by Chen and D'Zmura cannot be explained in this way. This also holds for the violations of the additive model found in our experiment, since we assured that all stimuli fulfilled the condition $F_i \geq 0$. The nature of this second type of violation is aptly described by Chen and D'Zmura in one particular example where a pink transparent overlay should have been seen in front of a gray background: "When the color of area 4 [**Q** in our notation] is made brighter than this gray, one sees immediately that area 4 is too bright to belong to a unitary percept of a transparent filter" (p. 602). As it happens, very similar stimuli were used in our experiment 1 (achromatic background, reddish layer). In Fig. 5 (top left), we can see that the additive model predicts a much higher luminance for **Q** than the scaling model for these stimuli. Our subjects consistently chose the prediction of the subtractive model and rated the stimulus as almost perfectly transparent. Conversely, this means that **Q** would appear as too bright if we chose the luminance predicted by the additive model, in line with the observation made by Chen and D'Zmura. Similar observations can be made in other reported cases. We may therefore conclude that the scaling model also avoids false predictions of this second type.

Our findings also have implications for Westland and Ripamonti's model (Westland & Ripamonti, 2000). They suggested that invariant cone-excitation ratios may be useful for defining the conditions of perceptual trans-

parency (ratio model). In a broad sense, we agree with this expectation, since this cue is indeed consistent with a special case of the scaling model. Our results indicate, however, that invariant cone-excitation ratios *as such* are probably not very useful as a cue for perceptual transparency. At least they are not a necessary condition for perceptual transparency, since many of the stimuli used in our experiments grossly violated the invariant-cone-excitation-ratio criterion but nevertheless elicited a compelling transparency impression. Indeed, qualitative observations suggest that the transparency impression is slightly less compelling in stimuli that conform to the invariant-cone-excitation-criterion than in stimuli that also share an additive component and therefore violate this criterion.

Scope of the Scaling Model

In our investigation we focused on stimuli that may plausibly be interpreted as resulting from a filter situation. For such stimuli, we found that the scaling model provides a more adequate description of the transparency conditions than both the additive model and the ratio model. Taking into account that the scaling model was designed to approximate color changes caused by optical filters, one could argue that the validity of the model is possibly restricted to stimuli that are compatible with a filter interpretation and that invalid predictions are to be expected in all other cases. However, this is in no way a necessary conclusion, because the scaling model is—despite its reference to filter situations—obviously not a model of physical filters but a psychophysical model that integrates basic properties of color changes that may result in situations where combinations of additive and subtractive color mixture take place. It is therefore quite possible that the scope of this model also includes stimuli that cannot be generated by a physical filter. An initial sign of this is that the scaling model does not exclude equiluminant stimuli, although such stimuli are normally not found in filter situations. One obtains such equiluminant stimuli, for example, if **A** is equiluminant to **B**, $\beta_L = \beta_M = 1/(1 + \kappa)$, $0 < \beta_S < 1$, and $\kappa \geq 0$. The scaling model is therefore—at least in principle—consistent with the finding that equiluminant stimuli may appear transparent (Chen & D'Zmura, 1998; D'Zmura et al., 1997). However, it remains an open empirical question whether all cases of equiluminant stimuli that appear transparent can be described by the scaling model. A similar point holds with respect to other physical situations that may evoke an impression of transparency, for instance, shadows and spot light illuminations. The image generation processes in these cases are not too different from that found in the filter situation, and therefore it seems reasonable to assume that there are at least specific forms of shadows and spot light illuminations that conform to the scaling model. Also in this case, it remains an open empirical question whether there are indeed shadows and spot light illuminations that are perceived as transparent but do not conform to the scaling model.

With respect to possible limits in the scope of the scaling model, it may be useful to consider the "generalized convergence model" proposed by D'Zmura et al (D'Zmura et al., 2000). It states that transparency should be perceived if $P_i = a_i A_i + T_i$, $Q_i = a_i B_i + T_i$, $0 < \alpha_i < 1$, $i = L, M, S$, holds. It is clear that, in a formal sense, both the additive and the scaling model are special cases of this generalized model, i.e., any colors **A**, **B**, **P**, **Q** that conform to the scaling model and any colors **A′**, **B′**, **P′**, **Q′** that conform to the additive model also conform to the generalized convergence model. A possible interpretation of the generalized convergence model could be that it includes a class of models that describe qualitatively different types of perceptual color scission and that the scaling model refers to just one of these types. The generalized convergence model may thus prove useful as a common theoretical framework for different models of color scission. However, it cannot serve as a replacement for specific models. This is clearly demonstrated by the results of this investigation, which show that even the true subset of solutions of the general model that conforms to the additive model contains many cases that do not appear transparent. We suspect that even the parameter restrictions formulated in the scaling model are too lenient and that further work is needed to refine these constraints.

Appendix A: Formulas

1. Prediction of the scaling model in Experiment 1

A, **B** are different achromatic colors, therefore $\mathbf{B} = s\mathbf{A}$, with $s \neq 1$. **P** is fixed to $\mathbf{P} = \alpha\mathbf{A} + (1 - \alpha)\mathbf{F}$ and per definition $\mathbf{Q} = \gamma\mathbf{B} + (1 - \gamma)\mathbf{F}$. Substituting these expressions for **B**, **P**, **Q** into Eq. (12) we get:

$$\kappa_i = \frac{2(Q_i A_i - P_i B_i)}{(P_i - Q_i)(A_i + B_i)} \tag{23}$$

$$= \frac{2[A_i s(\alpha - \gamma) + F_i(s - \alpha s + \gamma - 1)]}{(1 + s)[A_i(s\gamma - \alpha) + F_i(\alpha - \gamma)]}. \tag{24}$$

We search for a γ that solves the equations of the scaling model. This requires that $\kappa_i - \kappa_j = 0$, for $i, j = L, M, S$. This leads to

$$\frac{2Y_{ij}(s - 1)(\alpha + \alpha\gamma(s - 1) - \gamma s)}{(1 + s)X_i X_j} = 0, \tag{25}$$

with $Y_{ij} = A_i F_j - A_j F_i$ and $X_i = A_i(\gamma s - \alpha) + F_i(\alpha - \gamma)$. Since **A** is an achromatic and **F** a chromatic color it holds that $A_i/A_j \neq F_i/F_j$ and therefore $Y_{ij} \neq 0$ for at least one pair i, j. Furthermore, it holds that $(s - 1) \neq 0$ since $\mathbf{A} \neq \mathbf{B}$. Therefore we get the only possible solution for γ by solving

$$\alpha + \alpha\gamma(s - 1) - \gamma s = 0, \tag{26}$$

that is,

$$\gamma = \frac{\alpha}{\alpha + s - \alpha s}. \tag{27}$$

It must be checked separately whether this is a solution with admissible parameters for β_i and κ.

2. Predictions of the Additive and the Scaling Model in Experiment 2

If $\mathbf{A}$, $\mathbf{B}$, $\mathbf{P}$, and coordinate i of $\mathbf{Q}$ are fixed, then both models uniquely predict the values of Q_j, $j = L, M, S$, $j \neq i$, that solve the model equations. (A) Additive Model: With $\alpha = (P_i - Q_i)/(A_i - B_i)$ we get

$$Q_j = P_j - \alpha(A_j - B_j)$$

. (B) Scaling Model: First $\beta_i = (P_i - Q_i)/(A_i - B_i)$ and $W_i = (A_i + B_i)/2$ are calculated, then

$$\kappa = \frac{P_i - \beta_i A_i}{W_i \beta_i}. \tag{28}$$

We then get

$$\beta_j = P_j/(A_j + \kappa W_j) \tag{29}$$
$$Q_j = \beta_j(B_j + \kappa W_j) \tag{30}$$

It must be checked separately whether these are solutions with admissible parameters.

3. Correcting for Invalid Color Matching Functions

We used a colorimeter to calibrate the monitor that measures XYZ-values based on the color matching functions of the CIE 1931 2° standard observer. To convert XYZ-values displayed on the screen to cone excitations based on the 2° cone fundamentals provided by Stockman and SharpeStockman and Sharpe (2000) (and vice versa), we used the matrix:

$$M = \begin{pmatrix} 0.17156 & 0.52901 & -0.02199 \\ -0.15955 & 0.48553 & 0.04298 \\ 0.01916 & -0.03989 & 1.03993 \end{pmatrix} \tag{31}$$

(and its inverse M^{-1}), as proposed by Golz and MacLeod-Golz and MacLeod (submitted). The matrix is based on rescaled versions of the cone fundamentals $l(\lambda)$, $m(\lambda)$, $s(\lambda)$ given by Stockman and Sharpe, originally scaled to a peak value of 1: Golz and MacLeod first set $l'(\lambda) = 1.5l(\lambda)$ and then scaled $l'(\lambda)$, $m(\lambda)$ with $x = 0.4166013$ to ensure that $V^*(\lambda) = x[l'(\lambda) + m(\lambda)]$. In addition, they scaled $s(\lambda)$ with 1.915338. The authors show that the errors that result when this transformation is used to determine cone-excitations from XYZ values are less than 1% for typical monitor phosphors.

References

Allen, E. (1980). Colorant formulation and shading. In F. Grum & C. J. Bartelson (Eds.), *Optical radiation measurements. Vol 2: Color measurement.* New York: Academic Press.

Beck, J., & Ivry, R. (1988). On the role of figural organization in perceptual transparency. *Percept. Psychophys.*, *44*, 585–594.

Beck, J., Prazdny, K., & Ivry, R. (1984). The perception of transparency with achromatic colors. *Percept. Psychophys.*, *35*, 407–422.

Brainard, D. (1989). Calibration of a computer controlled monitor. *Color Res. Appl.*, *14*, 23-34.

Brill, M. (1984). Physical and informational constraints on the perception of transparency and translucency. *Vision Graph. Image Process.*, *28*, 356-362.

Chen, V. J., & D'Zmura, M. (1998). Test of a convergence model for color transparency. *Perception*, *27*, 595–608.

Da Pos, O. (1989). *Trasparenze*. Padova: ICONE s.r.l.

D'Zmura, M., Colantoni, P., Knoblauch, K., & Laget, B. (1997). Color transparency. *Perception*, *26*, 471–492.

D'Zmura, M., Iverson, G., & Singer, B. (1995). Probabilistic color constancy. In R. Luce, M. D'Zmura, D. Hoffman, G. Iverson, & R. Kimball (Eds.), *Geometric representations of perceptual phenomena.* (p. 187-202). Mahwah, NJ: Lawrence Erlbaum Assoc.

D'Zmura, M., Rinner, O., & Gegenfurtner, K. R. (2000). The colors seen behind transparent filters. *Perception*, *29*, 911-926.

Faul, F. (1996). Chromatic scission in perceptual transparency. *Perception*, *25* (Supplement), 105.

Faul, F. (1997). *Theoretische und experimentelle Untersuchung chromatischer Determinanten perzptueller Transparenz* (Ph.D. dissertation). Kiel, Germany: Christian-Albrechts-Universität zu Kiel.

Foley, J., van Dam, A., Feiner, S., & Hughes, J. (1990). *Computer graphics. principles and practice.* New York: Addision-Wesley.

Gerbino, W., Stultiens, C. I. F. H. J., Troost, J. M., & De Weert, C. M. M. (1990). Transparent layer constancy. *J. Exp. Psych.: Human Percep. & Perform*, *16*, 3–20.

Golz, J., & MacLeod, D. I. A. (submitted). Colorimetry for crt displays: almost-valid measures from invalid color matching functions and invalid assumptions. *Journal of Vision*.

Hagedorn, J., & D'Zmura, M. (2000). Color appearance of surfaces viewed through fog. *Perception*, *29*, 1169-1184.

Kasrai, R., & Kingdom, F. A. A. (2001). Precision, accuracy, and range of perceived achromatic transparency. *J. Opt. Soc. Am. A*, *18*, 1-11.

Maloney, L. (1986). Evaluation of linear models of surface spectral reflectance with small numbers of parameters. *J. Opt. Soc. Am. A*, *3*, 1673-1683.

Metelli, F. (1970). An algebraic development of the theory of perceptual transparency. *Ergonomics*, *13*, 59–66.

Metelli, F. (1974). The perception of transparency. *Sci. Am.*, *230*, 90–98.

Nakauchi, S., Silfsten, P., Parkinnen, J., & Usui, S. (1999). Computational theory of color transparency: recovery of spectral properties for overlapping surfaces. *J. Opt. Soc. Am. A*, *16*, 2612-2624.

Nascimento, S. M. C., & Foster, D. H. (1997). Detecting natural changes of cone-excitation ratios in simple and complex coloured images. *Proc. R. Soc. London Ser. B*, *264*, 1395-1402.

Parkkinen, J., Hallikainen, J., & Jaaskelainen, T. (1989). Characteristic spectra of Munsell colors. *J. Opt. Soc. Am. A*, *6*, 318-322.

Stiles, W. S., Wyszecki, G., & Ohta, N. (1977). Counting metameric object-color stimuli using frequency-limited spectral reflectance functions. *J. Opt. Soc. Am.*, *67*, 779–784.

Stockman, A., & Sharpe, L. T. (2000). Cone spectral sensitivities and color matching. In K. R. Gegenfurtner & L. T. Sharpe (Eds.), *Color vision. from genes to perception.* (p. 53-101). Cambridge University Press.

Westland, S., & Ripamonti, C. (2000). Invariant cone-excitation ratios may predict transparency. *J. Opt. Soc. Am. A*, *17*, 255–264.

Wyszecki, G., & Stiles, W. S. (1982). *Color science: Concepts and methods, quantitative data and formulae* (2nd ed.). New York: John Wiley and Sons.